Nonlinear analysis of steel scaffolds for shoring of concrete structures

http://dx.doi.org/10.1590/0370-44672014700009

Marcos Andrew Rabelo Soeiro
Professor Auxiliar II
Universidade de Fortaleza - Unifor
M.Sc. pela Universidade Federal do Ceará - UFC
Programa de Pós-Graduação em Engenharia Civil: Estruturas e Construção Civil
Fortaleza – Ceará - Brasil
neoandrew_ufc@hotmail.com

Aurea Silva de Holanda
Professora Associado II
Universidade Federal do Ceará - UFC
Departamento de Integração Acadêmica e Tecnológica em Engenharia e Arquitetura
Fortaleza – Ceará - Brasil
aurea@det.ufc.br

Evandro Parente Junior
Professor Associado III
Universidade Federal do Ceará - UFC
Departamento de Engenharia Estrutural e Construção Civil
Fortaleza – Ceará – Brasil
evandro@ufc.br

Abstract

Shoring systems are temporary structures that should resist external loads during the construction of concrete structures. Therefore, the shoring system should have sufficient strength and stiffness to ensure the safety of the concrete structure until it becomes self-supporting. Unfortunately, a large number of accidents occur during the construction of concrete structures due to the failure of the shoring system, showing the importance of improving the knowledge about these structures. This work aims to study the behavior of steel scaffolds used in the construction of high-clearance concrete structures using three-dimensional finite element models considering both geometrical and material nonlinearities. The obtained results are in good agreement with experimental results available in literature. The results showed that the boundary conditions have a significant influence on the failure loads of steel scaffolds.

Keywords: steel scaffolds, shoring systems, stability, nonlinear analysis.

1. Introduction

Shoring systems are temporary structures that should resist external loads during the construction of reinforced concrete structures and limit formwork deflections in order to ensure the quality of the built structure. They are subjected to external loads due to the weight of the formwork, fresh concrete, steel reinforcement, workers and construction equipment, as well as additional loads due to concrete pouring and vibration.

The construction industry uses several types of steel scaffolds with different geometries and connection types. This type of shoring system is used for high-clearance (generally higher than 4.5m) concrete structures. Steel scaffolds are generally built using lightweight steel tubes to facilitate transportation and handling. Hinged connections are widely used to simplify the assembly and disassembly of the scaffold at the building site.

Failure of shoring systems can cause deaths, injuries, construction delays, financial loss and other problems. Unfortunately, failure of shoring systems is a major cause of construction accidents in Brazil and other countries (Hadipriono, 1985; Peng *et al*., 1996; Soeiro, 2012). The accidents can be due to poor assembly, inadequate supports and design errors. As steel scaffolds are temporary structures used only during the construction phase, their analysis and design generally do not receive the same attention given to permanent structures. However, due to the large number of accidents registered throughout the world, the analysis and design of shoring structures has been receiving increasing attention (Peng *et al*., 1997; Weesner and Jones, 2001; Yu *et al*., 2004; Soeiro, 2012; Peng *et al*., 2013). In spite of this, the available literature dealing with steel scaffolds is still very limited.

Failure due to loss of stability is the main concern in the analysis and design of steel scaffolds, since they are mostly built using slender members loaded with compression. However, the use of simply linearized (eigenvalue) stability analysis, which is the standard practice, may not be adequate since steel scaffolds, as other shoring systems, generally present larger geometrical imperfections than permanent steel structures. These imperfections are caused by the manufacturing process, by damage during transportation and handling, and by inadequate assembly.

The analysis and design of steel

scaffolds is difficult, since the actual support conditions at the construction site are unknown. This article aims to present the structural behavior of shoring systems, as well as to discuss their safety assessment, in order to contribute to the safe design of this type of structure. To this end, the structural behavior of steel scaffolds will be studied using the Finite Element Method. It is important to note that, in most studies found in literature, the researchers only consider the geometrical nonlinearity (Yu *et al.*, 2004; Peng *et al.*, 2013).

Herein, both geometric and material nonlinearities will be considered in order to trace the equilibrium paths, study the post-buckling behavior, assess the imperfection sensitivity, and evaluate the load-carrying capacity of these structures. The geometric nonlinearity will be considered using a nonlinear finite element allowing large displacements and rotations, while the material nonlinearity considered uses an elasto-plastic constitutive model. The obtained results are compared with experimental and computational results available in literature. The influence of the boundary conditions in the post-buckling behavior and the load-carrying capacity are assessed.

2. Structural analysis

Steel scaffolds are built using slender tubular members and are loaded mostly under compression. However, as the applied load increases, transversal displacements and bending moments start to increase due to the presence of initial geometrical imperfections. Finally, the stresses caused by the combination of compression and bending lead to material failure by yielding. Therefore, in order to properly simulate the behavior of steel scaffolds from the beginning of the loading until failure, both geometrical and material nonlinearities should be considered.

In this study, the Finite Element Method (FEM) is applied to nonlinear analysis of steel scaffolds. Using the Virtual Work Principle, the nonlinear equilibrium equations of the finite element model can be written as:

$$\mathbf{r}(\mathbf{u}, \lambda) = \mathbf{g}(\mathbf{u}) - \lambda \mathbf{f} = \mathbf{0} \tag{1}$$

where $\mathbf{r}$ is the out-of-balance force vector (residual), $\mathbf{u}$ is the nodal displacement vector, $\mathbf{g}$ is the internal force vector, $\mathbf{f}$ is the reference load vector, and (λ) is the load factor. Thus, the external force vector is the product of the load factor (λ) by the reference force vector ($\mathbf{f}$).

The internal force vector of the FE model is assembled summing up the contributions of the internal force vector of each element. Using the Virtual Work Principle, the internal force vector of each element can be written as:

$$\mathbf{g} = \int_V \overline{\mathbf{B}}^t \sigma \, dV, \quad \overline{\mathbf{B}} = \frac{\partial \varepsilon}{\partial \mathbf{u}} \tag{2}$$

It is important to note that this expression allows the consideration of both geometric nonlinearity, through a displacement dependent $\bar{B}$ matrix, and material nonlinearity, through the nonlinear stress-strain relation $\sigma(\varepsilon)$.

The solution of nonlinear equilibrium equations can be carried-out using the Newton-Raphson Method (Crisfield, 1991). This is an iterative method based on the linearization of the nonlinear equations. It should be noted that Equation (1) describes a system of nonlinear equations with n+1 variables: n nodal displacements (degrees of freedom) plus the load factor (λ). One of the most important objectives of the nonlinear analysis is to evaluate the load-displacement curve, also known as the equilibrium path of the structure.

The Load Control Method is the simplest approach to trace the load-displacement curve. In this method, the load factor is increased by a fixed amount at the beginning of each step of a series of steps and kept fixed during the Newton-Raphson iterations, effectively eliminating one variable of the problem. The linearization of Equation (1) considering a fixed load factor (λ) leads to:

$$\mathbf{K}_T \delta \mathbf{u}_i = \lambda \mathbf{f}_i - \mathbf{g}_i \tag{3}$$

where i is the iteration counter, $\delta \mathbf{u}_i$ is the iterative correction of nodal displacements ($\mathbf{u}_{i+1} = \mathbf{u}_i + \delta \mathbf{u}_i$) and the tangent stiffness matrix ($\mathbf{K}_T$) is obtained by the linearization of Equation (2):

$$d\mathbf{g} = \frac{\partial \mathbf{g}}{\partial \mathbf{u}} d\mathbf{u} = \mathbf{K}_T d\mathbf{u} \tag{4}$$

with $\mathbf{K}_T = \mathbf{K}_E + \mathbf{K}_G$, where $\mathbf{K}_E$ is the material stiffness matrix and $\mathbf{K}_G$ is the geometric stiffness matrix (Bathe, 1995). The iteration process stops when the norm of the residual vector ($\|\mathbf{r}\|$) is smaller than a given tolerance.

Unfortunately, the Load Control Method can trace only the equilibrium path of stable structures, since the load factor is increasing in each step. On the other hand, the Arc-Length Method uses an additional constraint equation relating the increments of displacements ($\Delta \mathbf{u}$) and load factor ($\Delta\lambda$) leading to a system with n+1 equations and variables (Crisfield, 1991). This incremental-iterative method can be used to trace the complete equilibrium paths of structures presenting limit points, snap-through and snap-back (Crisfield, 1991).

The load-carrying capacity of a structure, i.e. the maximum load that the structure can carry without failure, is defined by the presence of critical points (limit or bifurcation) in the load-displacement curve (Crisfield,

1991). A limit point occurs when the load reaches a maximum (or minimum) and a bifurcation point occurs when two different equilibrium-paths (or branches) cross. Bifurcation points generally occur in perfect (i.e. ideal) structures, while most real-life (i.e. imperfect) structures reach the maximum load at limit points.

The tangent stiffness matrix ($\mathbf{K}_T$) is singular at critical points. For structures whose pre-buckling displacements are negligible, the condition of singularity of the stiffness leads to a generalized eigenvalue problem:

$$(\mathbf{K}_0 + \lambda \mathbf{K}_G)\,\mathbf{u} = \mathbf{0} \quad (5)$$

where $\mathbf{K}_0$ is the initial stiffness matrix (i.e. $\mathbf{K}_E(\mathbf{u} = \mathbf{0})$), $\mathbf{K}_G$ is the geometric stiffness matrix computed using the reference load vector ($\mathbf{f}$), the eigenvalues λ correspond to critical load factors and the eigenvectors $\mathbf{u}$ correspond to the critical modes (Bathe, 1995). The linearized buckling load is a good approximation of the failure load for perfect structures with high slenderness.

Unfortunately, initial geometric imperfections decrease the load-carrying capacity of the structure (Bazant and Cedolin, 1991). This aspect cannot be neglected in the present study since steel scaffolds can present large geometrical imperfections. These imperfections can be classified as global (out-of-plumbness) and local (member out-of-straightness). In the design of steel frames the global imperfections are the major concern since the local imperfections are accounted for in the compression member design provisions (AISC 360-10). According to AISC 360-10, the global imperfections can be considered through the use of equivalent horizontal loads, known as notional loads. For instance, in the analysis of permanent building frames:

$$F = \alpha P \quad (6)$$

where F are the notional loads, P are the vertical loads and $\alpha = 0.3\%$. This equation is associated with an initial out-of-plumbness of $h/333$, where h is the distance between the horizontal beams. The BS 5975:2008 also recommends the use of notional loads in analysis of the shoring system, but associated with larger imperfections (α = 1% to 2.5%), due to the temporary character of shoring structures, member damage during transportation and handling, and lower quality control of the assembly process.

It is important to note that steel scaffolds present both local and global imperfections whose actual shape and size are not known. However, the stability theory shows that the critical imperfections of columns and frames have the shape of the buckling modes (Bazant and Cedolin, 1991). The use of imperfections having the shape of buckling modes is also recommended by the AISC 360-10 standard. Therefore, in this work, geometric imperfection with the shape of the first buckling mode of the perfect structure has been used to study the structural behavior and evaluate the load-carrying capacity of steel scaffolds.

3. Numerical examples and discussion

The door-type modular steel scaffold shown in Figure 1 is studied herein, since it is widely used in Brazil and other countries. This structure was previously considered by Weesner and Jones (2001) and Yu *et al.* (2004) for both experimental and numerical investigations. Thus, the results obtained in this research are compared with the ones obtained by the cited authors to validate the computational models. It should be noted that these authors did not consider material nonlinearity and did not present the load-displacement curves, but only regarded the failure loads.

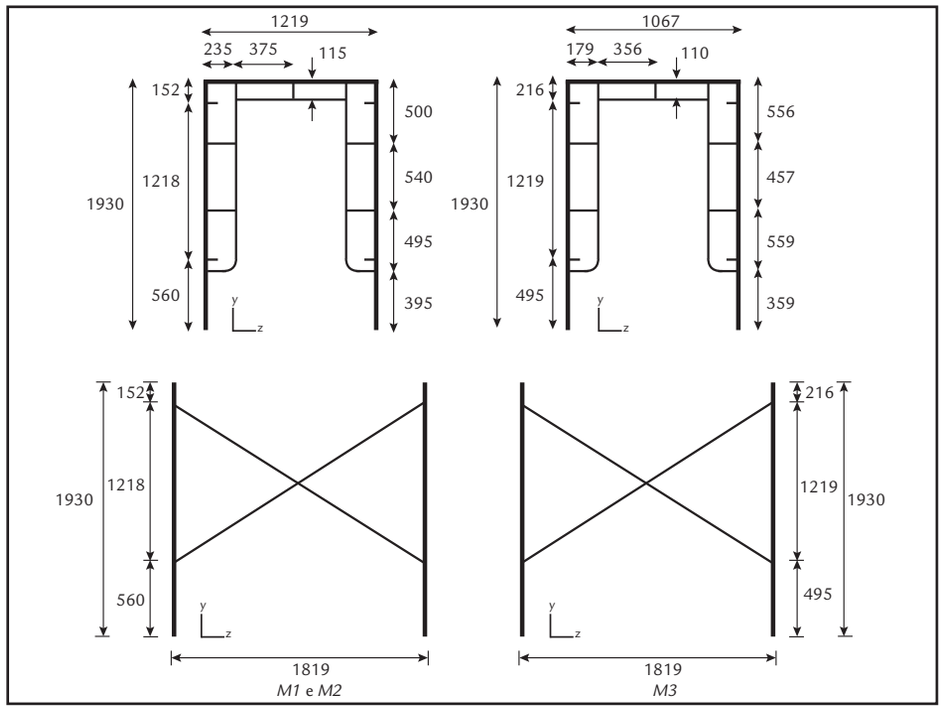

Figure 1
Typical Scaffold Frame Unit (Yu *et al.*, 2004).

Yu *et al.* (2004) built one, two and three-storey modular steel scaffolds and tested them until failure in order to investigate the structural behavior of multi-story door-type modular steel scaffolds. M1, M2 and M3 models were used for tests with one, two and three-story onebay modular steel scaffolds, respectively. In all tests, a vertical load was applied progressively with a 500kN hydraulic jack until unloading occurs. Results of the tests are presented in Table 1, where D represents the diameter, t is the thickness, P_t represents the maximum load applied per leg, E is the Young modulus and, finally, f_y is the yielding stress.

Models	D (main tube) mm	t (main tube) mm	D (internal tube) mm	t (internal tube) mm	P_t (kN)	f_y (N/mm²)	E (kN/mm²)
M1	43.3	2.67	26.6	1.6	63.4	406	205
M2	43.3	2.93	26.6	1.6	53.4	367	205
M3	43.0	2.40	32	2.1	45.2	402	205

Table 1
Results of experimental tests.

In the present work, a set of three-dimensional models was created in the commercial software ABAQUS (SIMULIA, 2007), using 3D frame elements based on the Euler-Bernoulli theory, in order to simulate the modular scaffolds of the experimental tests. These elements can accurately analyze framed structures with large displacement and rotations. Finite element meshes of 200, 400 and 600 elements were generated for M1, M2 and M3 models, respectively. In these models the connections between the door members were considered rigid, since they are welded together and the bracing diagonals are modeled as pinned. The connections between vertical members were also considered as rigid, since there is a large overlapping between internal and external tubes.

Initially, eigenvalue buckling analyses were performed to obtain the buckling loads and associated modes. After that, nonlinear analyses were performed in order to obtain the failure load and investigate the post-buckling behavior of the structure. Initial geometric imperfections with the shape of the first buckling mode and amplitude of 1% of the module height were considered in the nonlinear analysis. The adopted frame elements can handle large displacements and rotations. The material nonlinearity is considered using an elastic, perfectly plastic constitutive model with steel yielding stresses according to Table 1.

It is worthwhile to note that it is not easy to know the actual boundary conditions at the top and bottom of the steel scaffold. For this reason, different models were created, with distinct support conditions in order to investigate the influence of these conditions on the behavior of this type of structure. The four models are presented in Table 2.

Condition	Top						Base					
	Translational Constraint			Rotational Constraint			Translational Constraint			Rotational Constraint		
	X	Y	Z	Θx	Θy	Θz	X	Y	Z	Θx	θy	Θz
Pinned-fixed	Yes	No	Yes	No	No	No	Yes	Yes	Yes	Yes	Yes	Yes
Pinned-Pinned	Yes	No	Yes	No	No	No	Yes	Yes	Yes	No	No	No
Free-Fixed	No	No	No	No	No	No	Yes	Yes	Yes	Yes	Yes	Yes
Free-Pinned	No	No	No	No	No	No	Yes	Yes	Yes	No	No	No

Table 2
Boundary conditions of the steel scaffold.

4. Results and discussion

The buckling modes found in critical load analyses of M1, M2 and M3 models with different boundary conditions are illustrated in Figures 2, 3 and 4, respectively.

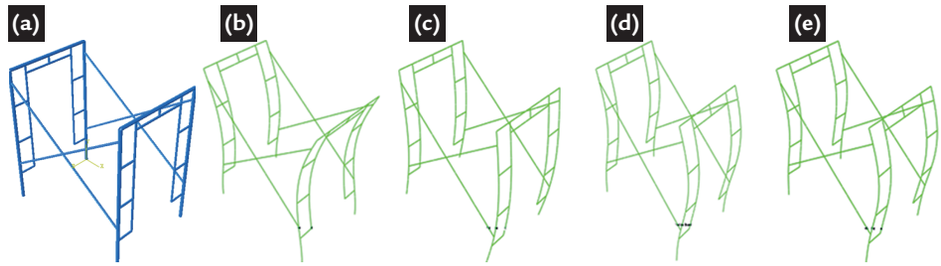

Figure 2
Buckling modes - M1 model.

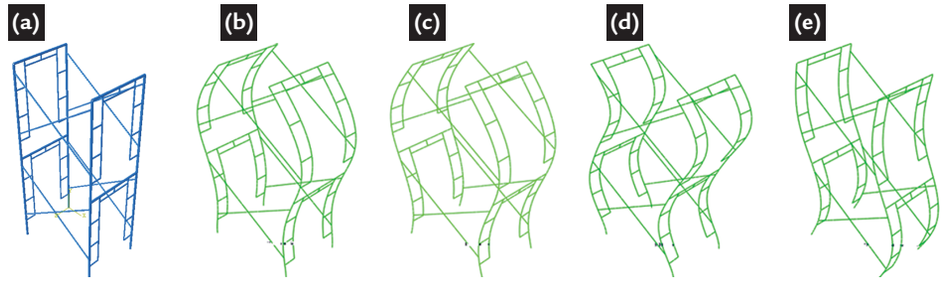

Figure 3
Buckling modes – M2 model.

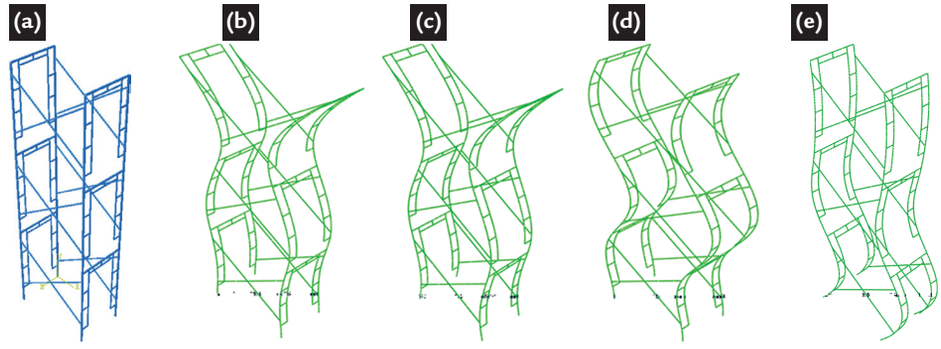

Figure 4
Buckling modes – M3 model.

Item (a) represents the undeformed scaffold, while (b), (c), (d) and (e) are the buckling modes for different boundary conditions. Item (b) corresponds to the deformed structure when a *free-fixed* boundary condition is considered, item (c) for a *free-pinned* condition, item (d) for a pinned-fixed condition, and, finally, item (e) corresponds to a pinned-pinned condition. These modes were used to define the initial imperfection for the nonlinear analyses and the critical loads are shown in Table 3. Beyond these analyses, purely geometric nonlinear analyses were performed and, finally, analyses were done considering the geometric and material nonlinearities together. Figures 5, 6 e 7 show load-displacement curves for M1, M2 and M3 model, respectively.

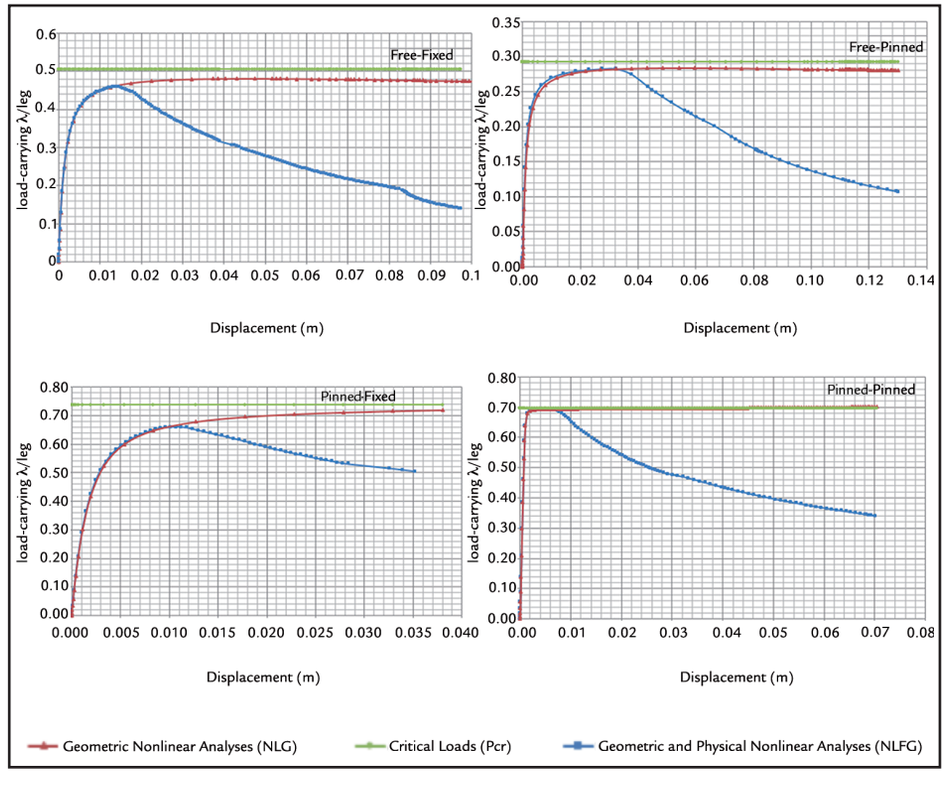

Figure 5
Load-displacement curves of the M1 model.

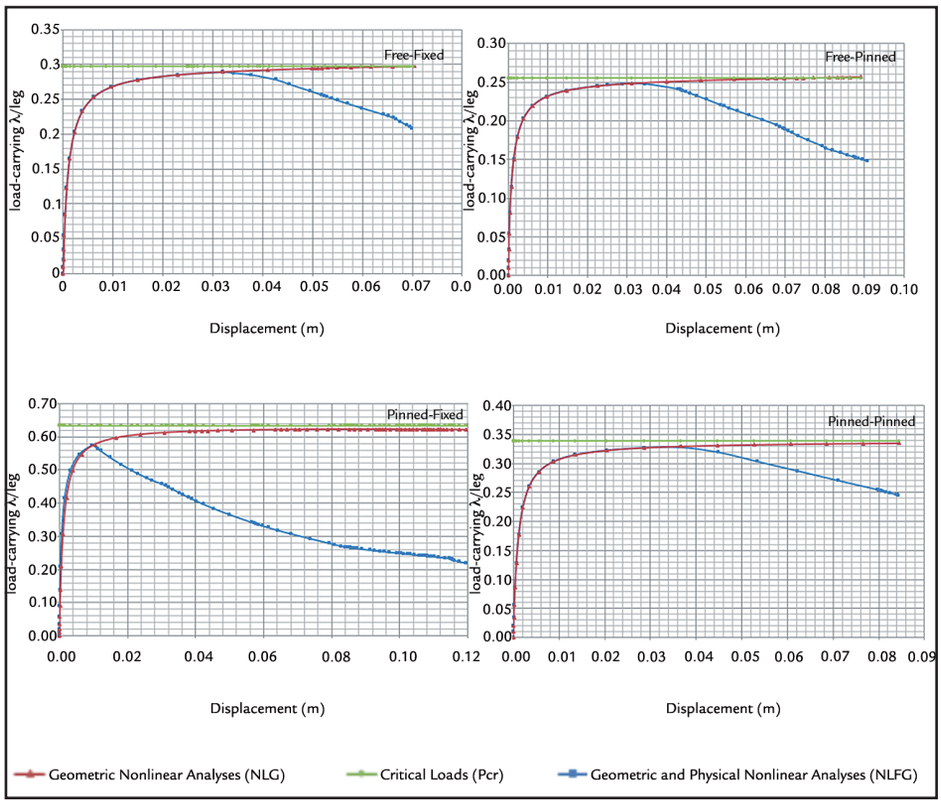

Figure 6
Load-displacement curves of the M2 model.

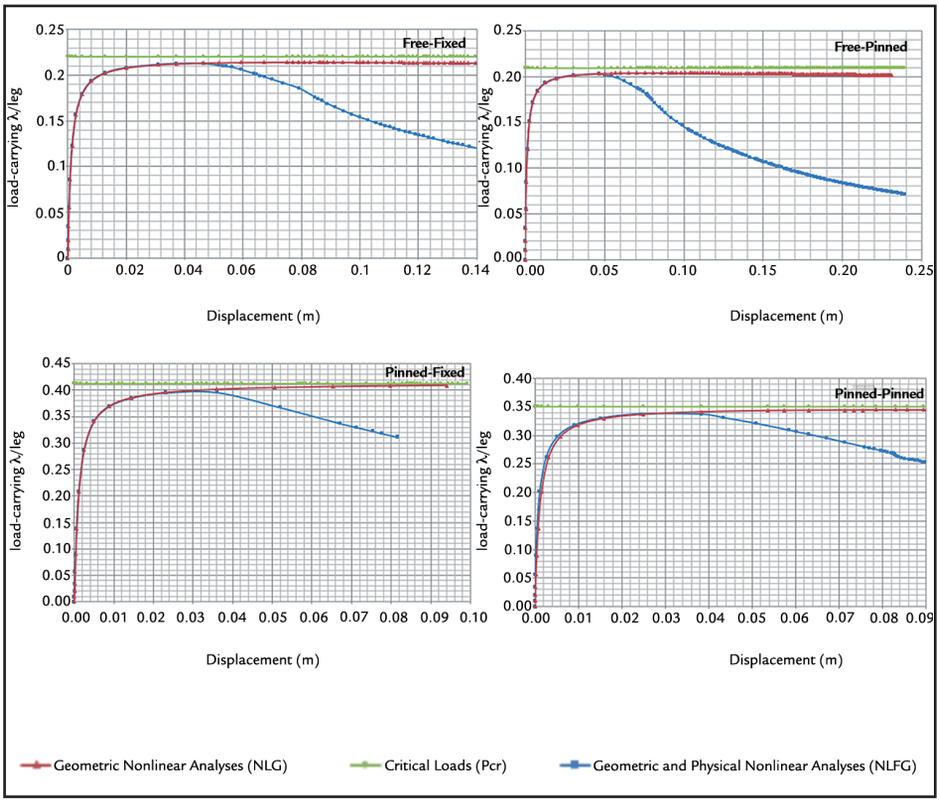

Figure 7
Load-displacement curves of the M3 model.

Table 3 presents the main results concerning the load-carrying capacity of the considered scaffolds. In this table, P_{cr} is the linearized buckling load, P_{NLGF} is the maximum load obtained considering material and geometrical nonlinearities, P_{NLG} is the maximum load considering only the geometrical nonlinearity, P_y represents the load where the scaffold begins to yield, P_t represents the experimental failure loads obtained by Yu *et al.* (2004) for M1 and M2 and by Weesner and Jones (2001) for M3, and P_n corresponds to the computational failure loads obtained by Yu *et al.* (2004). Additionally, two ratios are also presented in this table: $\chi = P_{cr}/P_t$ and $\gamma = P_{NLGF} / P_n$. The results obtained in this work are in good agreement with the ones obtained computationally by Yu *et al.* (2004), since in most of the 12 situations presented herein, the differences between them are inferior to 15%. It is important to note that Yu *et al.* (2004) considered only the geometric nonlinearity and used a different finite element discretization.

M1	P_{cr}	P_{NLG}	P_{NLFG}	P_y	P_n	P_t	χ	γ
Free –Fixed	63.217	60.09	57.51	57.16	54.8	63.4	0.997	1.05
Free-Pinned	36.564	35.49	35.32	35.32	32.5	63.4	0.58	1.09
Pinned-Fixed	92.191	89.89	82.54	82.03	69.7	63.4	1.45	1.18
Pinned-Pinned	86.947	86.95	86.83	86.69	66.3	63.4	1.37	1.31
M2	P_{cr}	P_{NLG}	P_{NLFG}	P_y	P_n	P_t	χ	γ
Free –Fixed	37.133	37.08	35.68	35.59	35.0	53.4	0.70	1.02
Free-Pinned	31.877	31.86	30.97	30.97	31.5	53.4	0.60	0.98
Pinned-Fixed	79.151	77.80	71.62	71.62	62.8	53.4	1.48	1.14
Pinned-Pinned	42.303	41.86	40.93	40.93	38.7	53.4	0.79	1.06
M3	P_{cr}	P_{NLG}	P_{NLFG}	P_y	P_n	P_t	χ	γ
Free -Fixed	27.553	26.79	26.58	26.58	30.3	45.2	0.61	0.88
Free-Pinned	26.221	25.54	25.40	25.40	29.3	45.2	0.58	0.87
Pinned-Fixed	51.618	51.12	49.49	49.49	45.6	45.2	1.14	1.09
Pinned-Pinned	43.864	43.08	42.16	42.11	41.6	45.2	0.97	1.01

Table 3
Failure loads (kN).

The P_{NLG} loads are always lower than the critical loads (P_{cr}) due to the geometrical imperfections. The loads P_{NLFG} are smaller than P_{NLG} due to yielding, with the difference between these loads depending on the boundary conditions. As expected, the critical load decreases with the increase in the number of modules when the same support condition is considered. An exception was found in the pinned-pinned condition, where a load decrease was observed when the number of modules changed from 3 (M3) to 2 (M2). This situation also occurred with the models used by Yu *et al.* (2004) and seems to be due to the differences of the associated buckling modes, as shown in Figures 3(e) and 4(e). In relation to the load carrying capacity, it is noted that the structure has low stress redistribution due to yield, since P_y is very close or equal to P_{NLGF}.

The results presented in Table 3 clearly show that boundary conditions have a significant influence in the load-carrying capacity of steel scaffolds. Thus, the ratio between the buckling and experimental failure loads (χ) varies from 0.58 to 1.45 in M1, from 0.60 to 1.48 in M2 and from 0.58 to 1.14 in M3. In addition, the ratio between the nonlinear and experimental failure loads (P_{NLFG} / P_t) varies from 0.56 to 1.37 in M1, from 0.58 to 1.34 in M2 and from 0.56 to 1.09 in M3, depending on the considered boundary conditions. It is important to note that the nonlinear failure loads (P_{NLFG}) are closer to the experimental ones than the simpler linearized buckling loads, which are generally used in practical applications.

5. Concluding remarks

The load-displacement curves considering only the geometric nonlinearity show that the scaffolds studied in this work present stable behavior with failure associated with large displacements. On the other hand, an unstable behavior with a clear limit point is obtained when the material nonlinearity is considered, explaining the catastrophic failure of these structures. Therefore, the consideration of the material nonlinearity is of paramount importance for the accurate simulation of the behavior of steel scaffolds. It is interesting to note that the imperfection sensitivity depends on the boundary conditions, in particular when the material nonlinearity is taken into account. However, generally this type of scaffold is not strongly imperfection sensitive.

The results obtained in this work show that the boundary conditions have a significant influence on the load-carrying capacity of steel scaffolds. However, the support conditions considered in the structural analysis are idealized, since the actual conditions on-site are rarely known. Thus, when the actual constraints at the top and/or base are not known, it is recommended to use the *free-pinned* condition, which is a conservative choice. The condition *pinned-pinned* should be used only if the falsework at the top of the scaffold is sufficiently stiff and its in-plane displacements are prevented by the existing concrete structure.

Acknowledgments

The authors would like to thank CNPq for the financial support received for the development of this research.

References

AMERICAN INSTITUTE OF STEEL CONSTRUCTION. ***AISC 360-10:*** specification for structural steel buildings. Chicago, 2010. 612 p.

BATHE, K. J. Finite element procedures. ***Revision of: Finite element procedures in engineering analysis,*** Prentice Hall, 1995.

BAZANT, Z. P., Cedolin L. ***Stability of structures: elastic, inelastic, fracture and damage theories.*** New York: Oxford University Press, , 1991.

BRITISH STANDARD INSTITUTION. ***BS 5975:*** code of practice for temporary works procedures and the permissible stress design of falsework. London, England: BSI, 2008.

CRISFIELD, M. A. ***Non-linear finite element analysis of solids and structures***. John Wiley and Sons, 1991. v.1.

HADIPRIONO, F. C. Analysis of events in recent structural failures. ***Journal of Structural Engineering,*** v.111, n. 7, p. 1468-1481, 1985.

PENG, J. L., PAN, A. D., ROSOWSKY, D. V., CHEN, W. F., YEN, T. High clearance scaffold systems during construction. Part I: Structural modelling and modes of failure. ***Engineering structures***, v. 18, n. 3, p. 247-257, 1996.

PENG, J. L., LIN, Y., WU, K. L., CHEN, W. F., YEN, T. Performance of scaffold frame shoring under pattern loads and load paths. ***Journal of Construction Engineering and Management,*** v. 123, n. 2, p. 138–145, jun. 1997.

PENG, J. L., WU, C. W., CHAN, S. L., HUANG, C. H. Experimental and numerical studies of practical system scaffolds. ***Journal of Constructional Steel Research,*** v. 91, p. 64-75, 2013.

SIMULIA. Abaqus user's manual, Version 6.7, 2007.

SOEIRO, M. A. R. ***Avaliação da segurança de torres metálicas para escoramentos de estruturas de concreto armado.*** Fortaleza: Universidade Federal do Ceará, Departamento de Engenharia Estrutural e Construção Civil, 2012. (Dissertação de Mestrado).

YU, W. K., CHUNG, K. F., CHAN, S. L. Structural instability of multi-storey door-type modular steel scaffolds. ***Engineering Structures,*** v. 26, n. 13, p. 867-881, 2004.

WEESNER, L. B., JONES, H. L. Experimental and analytical capacity of frame scaffolding. ***Engineering Structures,*** v. 23, n. 6, p. 592-599, 2001.

Received: 2 February 2014 - Accepted: 2 September 2016.